# Enhancement of the Electrical Properties of Poly(*p*-phenylene vinylene) by the Incorporation of Silicon Dioxide Nanoparticles

**Sook Yoon, Hyung-Ho Park**

*Department of Materials Science and Engineering, Yonsei University, 134 Shinchon-Dong, Seodaemun-Ku, Seoul, 120-749, Korea*

Received 17 September 2008; accepted 4 July 2009
DOI 10.1002/app.31084
Published online 23 March 2010 in Wiley InterScience (www.interscience.wiley.com).

**ABSTRACT:** The electrical properties of a poly(*p*-phenylene vinylene) (PPV) conjugated polymer using silver (Ag) as a cathode were improved by the incorporation of silicon dioxide ($SiO_2$) nanoparticles. The current density of the Ag–PPV/$SiO_2$ nanocomposite system was higher than that of Ag–PPV. A lower level of interfacial oxidation was found in the Ag–PPV/$SiO_2$ nanocomposite than in Ag–PPV, confirming that a more complete elimination of residue occurred in the nanocomposite. This was due to the relatively large surface area of the PPV/$SiO_2$ nanocomposite film and the hydrophilic surface of the $SiO_2$ nanoparticles. The lower level of oxidation contributed to an improvement in the material's current–voltage characteristics. Morphology-dependent current–voltage characteristics were enhanced by a large variation in the thickness of the Ag–PPV/$SiO_2$ nanocomposite film because an increased effective field strength could be induced in the thinner regions of the film. The incorporation of $SiO_2$ nanoparticles altered the effective film thickness and the amount of residue in the interior of the PPV without disrupting the structure of the conjugated polymer. The Ag cathode created a stable interface with the PPV film layer without causing the formation of an organic–metal complex, which would have obstructed electron injection. © 2010 Wiley Periodicals, Inc. J Appl Polym Sci 117: 700–705, 2010

**Key words:** conducting polymers; conjugated polymers; interfaces; nanocomposites; thin films

## INTRODUCTION

During the past 20 years, significant advances have been made in the performance of organic semiconductor materials used in various types of electronic devices.[1–6] Conjugated polymers are low-cost, possess a large area and excellent mechanical flexibility, and are simple to process. They have attracted interest in the applied sciences and technology because of their potential applications in organic semiconductor devices. There are, however, residues in most conjugated polymers. These residues cause conformational defects in conjugated polymer chains, which in turn obstruct carrier transport and degrade electrical properties.[7] Conjugated polymers are known to be unstable in air, suffering degradation upon exposure to oxygen and moisture. To compensate for these weak points, we have introduced inorganic nanoparticles into the conjugated polymer. The incorporation of inorganic nanoparticles into a conjugated organic semiconducting polymer can dramatically influence its electronic and optical properties,[8–11] although the mechanism of current enhancement in this material is not yet well understood.

Further development of polymer-based electronic devices requires a better understanding of their properties, such as the efficiency of light emission and its associated mechanism. The efficiency of these devices has been found to be highly dependent on the injection behaviors of the contacts, being limited primarily by the electron injection efficiency of the cathode.[12] Accordingly, substantial improvements in the electron injection efficiency require an in-depth study of interfaces with metal electrodes, including the morphologies and chemical reactions that occur at these interfaces. However, the physics of the charge-injection process is still not understood in detail. Low-work-function metals, such as calcium and magnesium, are susceptible to degradation by moisture and oxygen;[13] therefore, the moisture and

*Correspondence to:* H.-H. Park (hhpark@yonsei.ac.kr).

Contract grant sponsor: Basic Research Promotion Fund, Korean Ministry of Education and Human Resource Development; contract grant number: KRF-2006-311-D00636 (Korea Research Foundation Grant).

Contract grant sponsor: Ministry of Science and Technology (for the experiments at the Pohang Light Source).

Contract grant sponsor: Pohang University of Science and Technology (for the experiments at the Pohang Light Source).

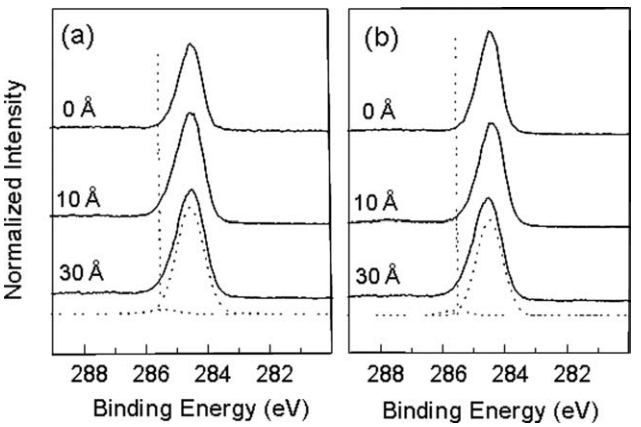


**Figure 1** $C_{1s}$ XPS core-level spectra of (a) PPV and (b) PPV/$SiO_2$ nanocomposite films with various amounts of Ag coverage (0, 10, and 30 Å thick). The dotted lines represent the line shapes with no Ag coating, and they were determined from deconvolution.

oxygen resistance of high-work-function metals may be advantageous for attaining a more stable electron injection cathode. Several studies have focused on using the properties of silver (Ag) to fabricate top-emitting organic light-emitting diodes.[14,15]

In this work, an organic semiconductor/metal electrode structure was designed with the combination of a poly(*p*-phenylene vinylene) (PPV)/silicon dioxide ($SiO_2$) nanocomposite organic layer for electron transport and a Ag electrode for the electron injection. We report on X-ray photoelectron spectroscopy (XPS), atomic force microscopy (AFM), and *in situ* near-edge X-ray absorption fine structure (NEXAFS) studies focusing on the effects of incorporating $SiO_2$ nanoparticles into the conjugated polymer PPV and on the formation of an interface between a PPV (or a PPV/$SiO_2$ nanocomposite) and a Ag electrode.

## EXPERIMENTAL

PPV was prepared with the sulfonium precursor route. The starting materials for the monomer were α,α′-dichloro-*p*-xylene and tetrahydrothiophene, and the monomer was then polymerized with sodium hydroxide (NaOH). The product was then dialyzed against water to eliminate monomer residues. To prepare the PPV film, the PPV precursor was spin-coated onto a clean indium tin oxide coated glass substrate and then thermally converted *in vacuo* at 200°C for 6 h. The PPV/$SiO_2$ nanocomposite precursor solution (0.2 wt % $SiO_2$ nanoparticle concentration for the PPV precursor) was prepared by the dispersion of the $SiO_2$ nanoparticles into the PPV precursors. The diameter of the $SiO_2$ nanoparticles was 7 nm. According to the product information, the $SiO_2$ nanoparticles used in this study have hydrophilic surface properties, and the surface moisture of the $SiO_2$ nanoparticles was almost completely eliminated by a heat treatment at 105°C for 2 h. The PPV/$SiO_2$ nanocomposite film was prepared with the same method used for the PPV film. For an interfacial bonding state analysis of the Ag–PPV and Ag–PPV/$SiO_2$ nanocomposite systems, a 10–30-Å-thick Ag layer was deposited onto the PPV and PPV/$SiO_2$ nanocomposite films under a pressure of $2 \times 10^{-5}$ Torr. XPS (Escalab 220i-XL, VG Scientific, West Sussex, England) was used with an Al Kα monochromatic source under $1 \times 10^{-9}$ Torr to analyze the chemical bonding state at the interface. *In situ* NEXAFS experiments were performed with a base pressure of $5 \times 10^{-10}$ Torr at the Pohang electron storage ring with a high-energy spherical grating monochromator beam line. The spectra were taken at an incident angle of 55°, the magic angle, to eliminate dependence on the polarization of the X-ray source. AFM (DI Dimension 3100, Digital Instruments, Plainview, NY) was used to observe the surface morphology of the film. For current–voltage measurements, three-layer devices, which consisted of an indium tin oxide coated glass substrate, a PPV (or PPV/$SiO_2$ nanocomposite) film, and an approximately 1500-Å-thick Ag layer deposited by e-beam evaporation, were prepared.

## RESULTS AND DISCUSSION

The XPS data for the $C_{1s}$, $Ag_{3d}$, and $O_{1s}$ core levels were collected to observe the evolution of the interfaces between the metal electrode and the organic layer according to the Ag thickness. These core

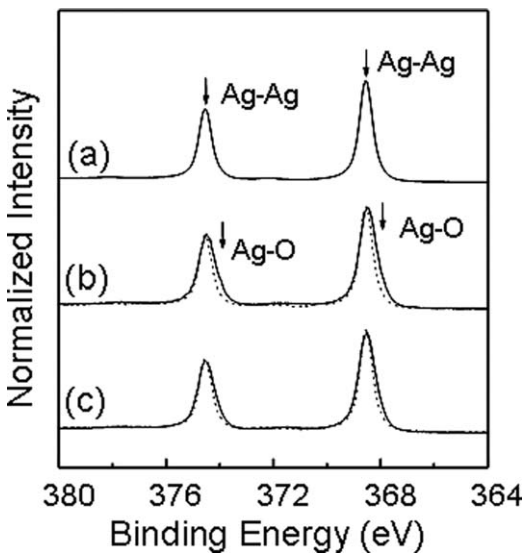


**Figure 2** $Ag_{3d}$ XPS core-level spectra of (a) pure Ag metal and (b,c) PPV and PPV/$SiO_2$ nanocomposite films, respectively, with 10 Å of Ag deposited. The dotted lines represent the line shapes of pure Ag metal, and they were determined from deconvolution.

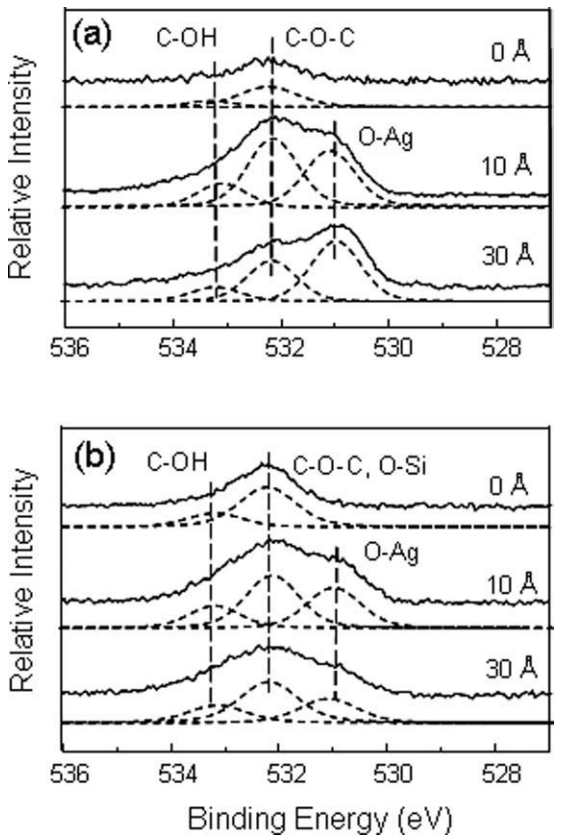


**Figure 3** $O_{1s}$ XPS core-level spectra of (a) PPV and (b) PPV/$SiO_2$ nanocomposite films with various amounts of Ag coverage (0, 10, and 30 Å thick). The dotted lines represent the constitutional bonding peaks determined from deconvolution.

levels are given in Figures 1–3 for the PPV and PPV/$SiO_2$ nanocomposite films. Figure 1 shows the development of the $C_{1s}$ core levels of the PPV and PPV/$SiO_2$ nanocomposite films as the Ag thickness increased. The $C_{1s}$ core-level spectra of the PPV film showed a major peak associated with the C—C/H species (C bonds mainly with C but also with H) and a minor peak associated with the C—O/OH at the shoulder. However, the minor peak appeared as a weak trace. Most oxygen-containing species originate from the inner part of a bulk conjugated polymer because thermal conversion usually incompletely eliminates residues such as moisture and oxygen in PPV and PPV/$SiO_2$ nanocomposite films. After the deposition of Ag on the PPV and PPV/$SiO_2$ nanocomposite films, the peak shape became slightly asymmetric. This is indicated by the dotted lines in the figure. Figure 1 shows traces related to an oxidized interface. This indicates that the degree of interfacial interaction of both the Ag–PPV and Ag–PPV/$SiO_2$ nanocomposite systems was relatively low because of the high chemical stability of Ag. Interactions at the interfaces between the Ag and the PPV or PPV/$SiO_2$ nanocomposite systems were weak in comparison with those at other metal–PPV interfaces. The adsorbed oxygen and residual moisture may have been drawn from the inside of the PPV and PPV/$SiO_2$ nanocomposite to the interface during Ag deposition because of the heat of condensation of the Ag and the heat of formation of the silver oxides. The XPS analysis of the $C_{1s}$ spectra showed a similar trend for the interfacial chemical reactions for both the PPV and PPV/$SiO_2$ nanocomposite films with Ag. Although it was not easy to find evidence of interfacial oxidation through the XPS study, a difference in the degree of interfacial oxidation between the Ag–PPV and Ag–PPV/$SiO_2$ nanocomposite systems was measured. This difference was also observed with *in situ* NEXAFS analysis.

The $Ag_{3d}$ XPS core-level spectra of pure Ag metal, Ag on PPV, and Ag on PPV/$SiO_2$ nanocomposite films are shown in Figure 2. The PPV and PPV/$SiO_2$ nanocomposite films with 10 Å of deposited Ag produced similar spectra. The $Ag_{3d}$ core-level spectra for both systems showed an extra bonding state of Ag—O at a lower binding energy than in metallic Ag.[16] It is known that the peak originating from the Ag—O bond appears at a lower binding energy than the bond in a pure, metallic Ag state.[16] The dotted lines in Figure 2(b,c) correspond to the metallic $Ag_{3d}$ of pure Ag metal. Interfacial oxidation was confirmed by the differences between the solid and dotted lines. The difference in the $Ag_{3d}$ core-level spectra between the Ag–PPV and the pure Ag metal was a little greater than that in the case of the Ag–PPV/$SiO_2$ nanocomposite. This indicated that slightly more oxidation occurred at the Ag–PPV interface.

The $O_{1s}$ XPS spectra of the Ag–PPV and Ag–PPV/$SiO_2$ nanocomposite systems are shown in Figure 3. Before the deposition of Ag onto the PPV or PPV/$SiO_2$ nanocomposite films, the $O_{1s}$ peak contained two component peaks, C—O—C and C—OH. However, after the deposition of Ag onto the pristine films, a peak associated with the O—Ag bond was generated. During the deconvolution, the peak binding energy, peak shape (Gaussian/Lorentzian ratio), and full width at half-maximum of each constitutional peak were kept constant. Before the deposition of Ag, the relative intensity of the $O_{1s}$ peak of the pristine PPV/$SiO_2$ nanocomposite film was stronger than that of the pristine PPV film. This was due to the contribution of O—Si bonds in the $SiO_2$ nanoparticles, which had almost the same binding energy as the C—O—C bond.[17] As expected, the $O_{1s}$ peak shapes of the Ag–PPV and Ag–PPV/$SiO_2$ nanocomposite systems were nearly the same with respect to Ag deposition. However, the two systems differed in the generation of oxygen bonds: the number of newly formed oxygen bonds in the Ag–PPV system was much larger than that in the Ag–PPV/$SiO_2$

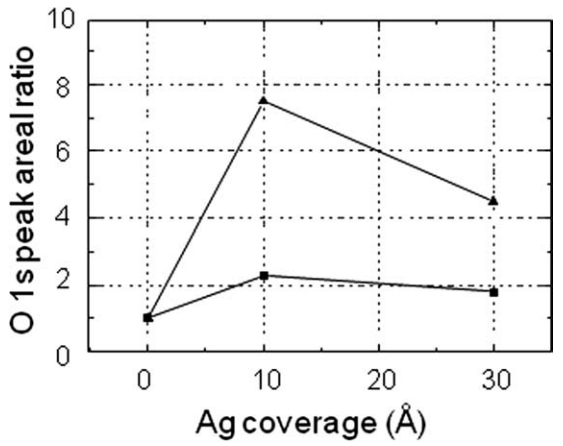


**Figure 4** $O_{1s}$ peak area ratios of the Ag-deposited films to the pristine films with various amounts of Ag coverage (0, 10, and 30 Å thick) for (▲) PPV and (■) PPV/$SiO_2$ nanocomposite films.

nanocomposite system. After the deposition of 10 Å of Ag onto the PPV, the relative intensity of the $O_{1s}$ peak increased abruptly at the Ag–PPV interface in comparison with the increase at the Ag–PPV/$SiO_2$ nanocomposite interface. After the deposition of 30 Å of Ag, the relative intensity of the $O_{1s}$ peak decreased slightly in the Ag–PPV and Ag–PPV/$SiO_2$ nanocomposite systems. For both systems, the decrease in the $O_{1s}$ peak intensity was due to the thick metal overlayer.

Figure 4 shows that there were more active interactions, such as oxidation, in the Ag–PPV system than in the Ag–PPV/$SiO_2$ nanocomposite system. After the deposition of 10 Å of Ag, the ratio of the $O_{1s}$ peak area to that of the initial state increased abruptly. The increased size of the $O_{1s}$ peak area with increased Ag deposition thickness obviously resulted from oxidation at the Ag–organic layer interface. Consequently, it is likely that the abrupt change at the Ag–PPV interface was caused by the presence of more residues, such as moisture and oxygen, in the PPV film versus the PPV/$SiO_2$ nanocomposite film. These residues could be drawn to the interface during the deposition of Ag by the heat of condensation of Ag and the heat of formation of Ag—O bonds. After the deposition of 30 Å of Ag, the decreasing ratio of $O_{1s}$ was attributed to the relative increase in the metal overlayer.

The reason for the presence of fewer residues, such as oxygen and $OH^-$ species, in the PPV/$SiO_2$ nanocomposite film versus the PPV film is that $SiO_2$ nanoparticles assisted in the elimination of residues from the film during thermal conversion. The conjugated polymer PPV tended to trap moisture and oxygen species during synthesis and thermal conversion.[18] The $SiO_2$ nanoparticles for the PPV/$SiO_2$ nanocomposite film had hydrophilic properties. While the PPV/$SiO_2$ nanocomposite precursor was stirred to ensure good dispersion, the surfaces of the $SiO_2$ nanoparticles attracted moisture, such as $OH^-$ species, to the PPV/$SiO_2$ nanocomposite. Well-dispersed $SiO_2$ nanoparticles in the precursor likely promoted a decrease in the amount of water trapped in the PPV polymer chains. The elimination of moisture from the nanocomposite, which could originate at the surface of $SiO_2$ nanoparticles, was easier than the removal of moisture trapped in the conjugated polymer PPV.[19] Consequently, the $SiO_2$ nanoparticles played an important role in the elimination of residues from the PPV/$SiO_2$ nanocomposite.

AFM images were taken at 3 × 3 to demonstrate changes in the film surface morphology after the introduction of $SiO_2$ nanoparticles (Fig. 5). The root mean square roughness was measured as 15 and 311 Å for the PPV and PPV/$SiO_2$ nanocomposite films, respectively. The surface of the PPV/$SiO_2$ nanocomposite film was much rougher than that of the PPV film because of the presence of $SiO_2$

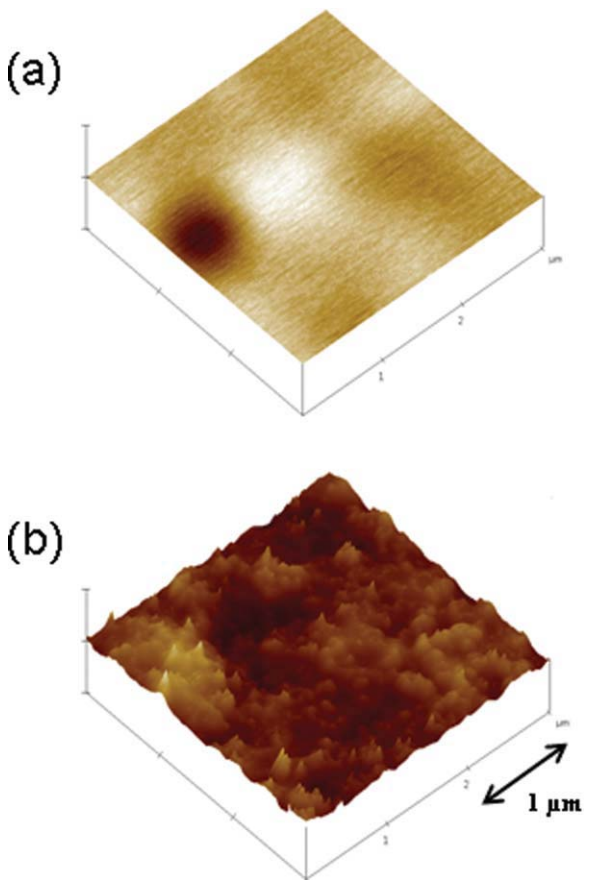


**Figure 5** AFM images of the surface morphology of (a) PPV and (b) PPV/$SiO_2$ nanocomposite films.[17] [Color figure can be viewed in the online issue, which is available at www.interscience.wiley.com.]

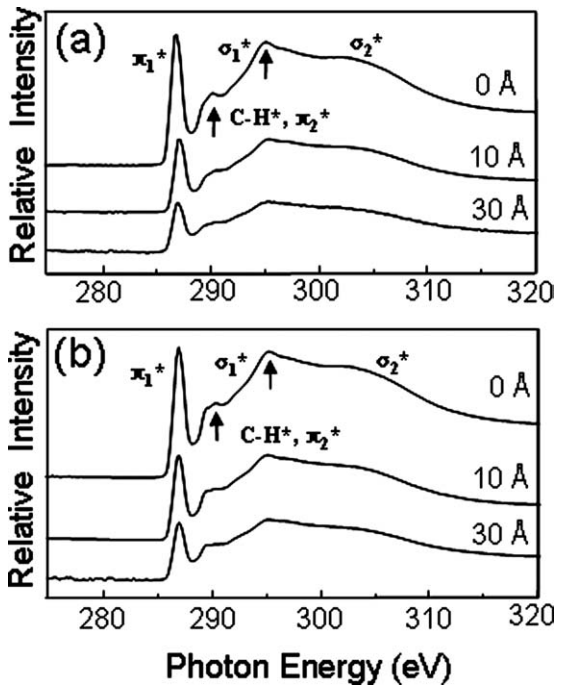


**Figure 6** Carbon K-edge NEXAFS spectra of (a) PPV and (b) PPV/$SiO_2$ nanocomposite films with various amounts of Ag coverage (0, 10, and 30 Å thick).

nanoparticles. The rougher surface resulted in regions in which the film thickness of the PPV/$SiO_2$ nanocomposite was much smaller than that of the PPV; the electron flow through the PPV/$SiO_2$ nanocomposite film was enhanced at these locations.

The NEXAFS spectra at the carbon K-edge following the deposition of Ag onto the PPV and PPV/$SiO_2$ nanocomposite films are given in Figure 6. For the pristine PPV, a sharp resonance can be seen near 287 eV due to a direct transition of the $C_{1s}$ core-level electron to $\pi_1^*$. The spectral features near 290 eV are the C—H* and $\pi_2^*$ structures. The two broad features beyond 293 eV are assigned to $\sigma_1^*$ and $\sigma_2^*$ regions.[20] Similar features were observed in the carbon K-edge NEXAFS spectrum of the pristine PPV/$SiO_2$ nanocomposite. This indicates that there was no destructive interaction of the PPV conjugated polymer backbone in the PPV/$SiO_2$ nanocomposite resulting from the introduction of $SiO_2$ nanoparticles. Upon Ag deposition onto the PPV and PPV/$SiO_2$ nanocomposite films, the positions and shapes of the peaks remained unchanged. The NEXAFS peak intensities of the PPV and PPV/$SiO_2$ nanocomposite structures became weak because of the increase in the Ag overlayer. After the deposition of 10 Å of Ag, the features that originated from the PPV and PPV/$SiO_2$ nanocomposite structures were still dominant. Even after the Ag thickness increased to 30 Å, the features indicating the respective characteristics of the PPV and PPV/$SiO_2$ nanocomposite structures were still distinguishable. In other words, there were no strong shifts and no prominent new features after Ag deposition. This indicates that the interfacial interactions between the Ag overlayer and the films were not accompanied by strong chemical bond formation, such as the formation of an organic–metal complex. Thus, there was no change in the molecular orbital structures of the PPV and PPV/$SiO_2$ nanocomposites.

To investigate the effect of $SiO_2$ nanoparticles on the electrical properties of Ag devices, the current–voltage characteristics for both systems were measured. In Figure 7, the current–voltage curves of devices with the Ag–PPV and Ag–PPV/$SiO_2$ nanocomposites are given. The current density of the device containing the $SiO_2$ nanoparticles was much higher than that of the device without them. Also, the electrical turn-on voltage of the device containing the PPV/$SiO_2$ nanocomposite was lower than that of the device containing PPV. These results indicate that the incorporation of $SiO_2$ nanoparticles into PPV effectively improves its current–voltage characteristics. We believe that the elimination of residues led to an increase in the electron injection area and a decrease in the effective thickness of the PPV/$SiO_2$ nanocomposite film because of increased surface roughness.

The elimination of residues during the deposition of Ag caused reduced interfacial interaction at the interface between the Ag overlayer and the PPV/$SiO_2$ nanocomposite film in comparison with that at the interface between the Ag and PPV film. This led to a higher current density in the Ag–PPV/$SiO_2$ nanocomposite system. The effective elimination of residues promoted efficient electron transport in the conjugated polymer PPV. On the basis of these observations, we conclude that a more complete

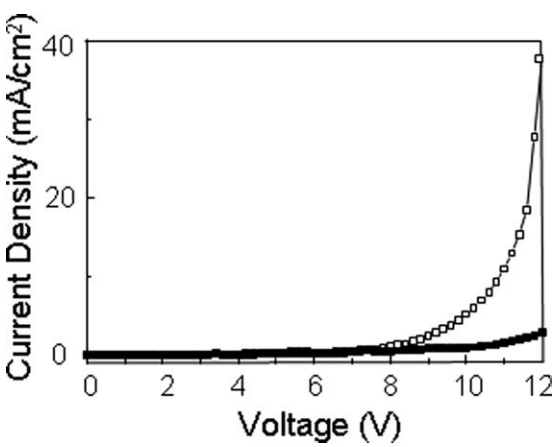


**Figure 7** Current–voltage characteristics for (■) Ag–PPV and (□) Ag–PPV/$SiO_2$ nanocomposite systems.

elimination of residues and a rougher surface resulting from the introduction of $SiO_2$ nanoparticles were the main causes of the improvements in the current–voltage characteristics of the Ag–PPV/$SiO_2$ nanocomposite system.

## CONCLUSIONS

By focusing on the presence of $SiO_2$ nanoparticles, we have demonstrated that the enhanced current density in the Ag–PPV/$SiO_2$ nanocomposite was influenced by both the surface morphology and the amount of residue present. The interfacial analyses of Ag–PPV systems with XPS and *in situ* NEXAFS revealed that there was a difference in the amount of residues present in the PPV and PPV/$SiO_2$ nanocomposite films, and this caused a difference in the degree of interfacial reactions in the two systems. Less residue was present after the incorporation of $SiO_2$ nanoparticles because of their hydrophilic surfaces and a relatively large surface area resulting from the rough surface morphology of the PPV/$SiO_2$ nanocomposite film. This led to improved current–voltage characteristics and an increase in the effective applied field strength at the thinner parts of the film, which resulted from a rough surface morphology. However, for real applications to optoelectronic devices, smaller sizes and the amount of nanoparticle incorporation should be considered to obtain an appropriate surface roughness for proper device performance.

## References


1. Yu, G.; McElvain, J.; Heeger, A. J. Adv Mater 1998, 10, 1431.
2. Halls, J. J. M.; Pichler, K.; Friend, R. H.; Moratti, S. C.; Holmes, A. B. Appl Phys Lett 1996, 68, 3120.
3. Burroughes, J. H.; Jones, C. A.; Friend, R. H. Nature 1988, 335, 137.
4. Tang, C. W.; VanSlyke, S. A. Appl Phys Lett 1987, 51, 913.
5. Burroughes, J. H.; Bradely, D. D. C.; Brown, A. R. Nature 1990, 347, 539.
6. Friend, R. H.; Gymer, R. W.; Holmes, A. B. Nature 1999, 397, 121.
7. Martens, H. C. F.; Blom, P. W. M.; Schoo, H. F. M. Phys Rev B 1996, 61, 7489.
8. Arango, A. C.; Carter, S. A.; Brock, P. J. Appl Phys Lett 1987, 74, 1698.
9. Carter, S. A.; Scott, J. C.; Brock, P. J. Appl Phys Lett 1997, 71, 1145.
10. Hide, F.; Schwartz, B. J.; Diaz-Garcia, M. A.; Heeger, A. J. Chem Phys Lett 1996, 256, 424.
11. Kumar, N. D.; Joshi, M. P.; Friend, C. S.; Prasad, P. N.; Burzynski, R. Appl Phys Lett 1997, 71, 1388.
12. Yan, L.; Mason, M. G.; Tang, C. W.; Gao, Y. Appl Surf Sci 2001, 175, 412.
13. Lee, D. W.; Kim, K.; Jin, J.-I.; Park, Y. Synth Met 2004, 143, 181.
14. Wu, Z.; Chen, S.; Yang, H.; Zhao, Y.; Hou, J.; Liu, S. Semicond Sci Technol 2004, 19, 1138.
15. Hao, X. T.; Zhu, F. R.; Ong, K. S.; Tan, L. W. Semicond Sci Technol 2006, 21, 19.
16. Bao, X.; Muhler, M.; Schedel-Niedrig, T.; Schlogl, R. Phys Rev B 1996, 54, 2249.
17. Yoon, S.; Yoon, K. H.; Park, H.-H. J Electroceram 2008, 21, 752.
18. Vaeth, K. M.; Jensen, K. F. Macromolecules 1998, 31, 6789.
19. Yokoyama, R.; Suzuki, S.; Shirai, K.; Yamauchi, T.; Tsubokawa, N.; Tsuchimochi, M. Eur Polym J 2006, 42, 3221.
20. Ettedgui, E.; Razafitrimo, H.; Gao, Y. Phys Rev Lett 1996, 76, 299.